

Shannon Entropy Helps Optimize the Performance of a Frequency-Multiplexed Extreme Learning Machine

MARINA ZAJNULINA^{1,*}

¹Multitel Innovation Centre, Rue Pierre et Marie Curie 2, Mons, 7000 Belgium

*zajnulina@multitel.be

Compiled August 15, 2024

Knowing the dynamics of neuromorphic photonic schemes would allow their optimization for controlled data-processing capability at possibly minimized energy consumption levels. In nonlinear substrates such as optical fibers or semiconductors, these dynamics can widely vary depending on each optical input encoded with information to process and are in general difficult to estimate. Thus, other approaches are required to optimize the schemes. Using a frequency-multiplexed fiber-based Extreme Learning Machine as an example for a classification task, I use Shannon entropy for optical power and introduce Shannon entropy for optical phase and spectrum, all averaged only over a small subset of the dataset to process. I show that the maximum and upper moderate optical power and phase entropies relate to the best data-processing capability of the Machine and, thus, can be used to find optimal system parameters such as fiber length, input power, and group-velocity dispersion in a more time-efficient manner than running numerical simulations emulating the scheme. Shannon entropy of the spectrum provides the information for what parameter space broadest possible frequency combs can be expected and is interesting from the perspective of frequency comb and supercontinuum generation. The introduced entropies are general and can be easily applied to describe and optimize other neuromorphic-photonic or nonlinear-optics schemes.

<http://dx.doi.org/10.1364/ao.XX.XXXXXX>

Introduction. Due to their ultra-wide bandwidths ranging up to tens of THz, comparably low energy consumption, and inherent analog nature, neuromorphic photonic schemes constitute promising candidates to surpass the data-processing capabilities of the state-of-the-art electronic computing devices built upon von Neumann architecture. They utilize light as the information carrier. Light has multiple degrees of freedom, such as amplitude, frequency (or wavelength), phase, modes, and polarization, offering the possibility of parallel data processing via various multiplexing techniques [1], [2], [3].

There are two major types of such schemes being under study. The first type is the so-called Reservoir Computers that consti-

tute neuromorphic counterparts of recurrent neural networks (cf. [4]). The second type is the Extreme Learning Machines (ELMs) constituting feed-forward neural networks. In ELMs, the connections between the input and hidden layer remain untrained, only the connections between the hidden and output layer undergo a training procedure which often happens using (ridge) linear regression [5], [6]. The nonlinearity needed to transform the input data in the hidden layer is often simply the optical nonlinearity of the medium through which light modulated with information is propagating; other types of nonlinearity such as, for instance, the nonlinearity of the read-out photodiodes can also be exploited (cf. [7]). Successful propositions and implementations of ELMs that use continuous spectra for data encoding and the subsequent transformation in optical fibers by Kerr nonlinearity are reported in Refs. [8], [9]. Ref. [10] utilizes low levels of second and third (Kerr) nonlinearity in a Lithium Niobate waveguide pumped with pulses of the order of tens of pJ. Ref. [11] deploys the Kerr-nonlinearity-based coupling between the modes of a multi-mode fiber in their feed-forward neural network similar to an ELM at remarkable low-power consumption levels (50 nJ pulses with an average power of 6.3 mW).

Although the optical nonlinearities deliver promising results for neuromorphic photonic schemes, the question of the correlation or even dependence between their internal nonlinear dynamics and data-processing performance is hardly asked. Instead, these schemes are often treated as black boxes. However, this question is essential from the point of view of optimization and control. Thus, the answer to it might lead to a further decrease in power consumption and simplified system designs with controllable data-processing capabilities. Admittedly, the question of internal dynamics is not easy to address, in particular, because the encoded optical inputs lead to a wide range of possible dynamical regimes in the guiding medium for the same system parameters, all depending on the sample values encoded. So, other approaches are needed that might allow for the optimization and control of neuromorphic photonic schemes without knowing their precise dynamics.

As photonic neuromorphic schemes can be considered as high-dimensional nonlinear dynamical systems, Shannon entropy - known as an effective dynamical indicator ([13]) - comes into question to relate the system's internal dynamics and its performance. It is a measure of the information content of a system. Information, on the other hand, is the statistical notion of how unlikely it is an event. Thus, unlike events coincide with

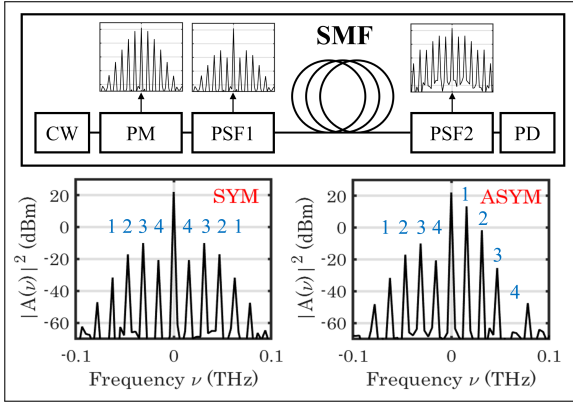


Fig. 1. *Top:* Experimental realization of a frequency multiplexed Extreme Learning Machine with CW: continuous-wave laser, PM: phase modulator, PSF1: programmable spectral filter 1, SMF: standard single-mode fiber, PSF2: programmable spectral filter 2, and PD: photo diode [12]. *Bottom:* Symmetric (SYM) and asymmetric (ASYM) information encoding by PSF1.

high information. Generally, dynamical systems either conserve (constant entropy) or destroy information (decreasing entropy) [14]. The entropy of a data-processing system can increase [15]. Originally formulated via probabilities, Shannon entropy has now extended to fields and absolute values (powers) [16], [17].

Here, I consider a fiber-based frequency-multiplexed ELM that utilizes frequency combs for encoding and processing input information (Fig. 1 (top), [12]). Two types of information encoding, symmetric (SYM) and asymmetric (ASYM) in the amplitudes of the comb lines (Fig. 1 (bottom)), are considered. Using the notion of Shannon entropy for the optical power ([16]) as well as introducing Shannon entropy for the optical phase and spectrum, I show that these quantities allow for a quick estimation of the ELM optimal parameters without knowing the precise dynamics. Maximal and upper moderate entropy in the optical power and phase allows for finding the optimal ELM fiber length and input power, as well as choosing a more effective information encoding type. Thus, I found that the ELMs optimal fiber length is $L = 1$ km (longer than in Ref. [12]), the input power is $P = 0.27$ W (lower than in Ref. [12]). Further, the input information should be encoded asymmetrically in the comb line amplitudes (similar to Ref. [12]) rather than symmetrically. The introduced entropies are general and can be applied to other neuromorphic schemes and configurations. In particular, Shannon entropy of the spectrum can be deployed by the nonlinear optics community to find system parameters for broad optical frequency combs.

Methods. The experimental realization and validation of the fiber-based frequency-multiplexed ELM (Fig. 1, top) is reported in Ref. [12]. The ELM input layer consists of a continuous-wave laser (CW) in the C band, a phase modulator (PM), and a programmable spectral filter (PSF1) that are used to generate an initial frequency comb to subsequently encode the input information by attenuating its lines with values corresponding to the features of the dataset samples. The hidden layer is a standard single-mode fiber (SMF) in which the modified (modulated) comb is transformed under the impact of the Kerr nonlinearity. The read-out layer consists of a second programmable spectral filter (PSF2) and a photodiode (PD) to collect the comb line in-

intensities one by one. The vectors of the comb-line intensities are stuck into a matrix that is used for linear regression to generate an ELM prediction. A similar approach is proposed and numerically studied in Ref. [18]. Whereas the latter system operates in a highly nonlinear regime utilizing a high-power CW laser as a source and a highly nonlinear fiber (HNLNF) as a Kerr medium, the ELM in Ref. [12] effectively processes data at low Kerr nonlinearity at an average power of only 0.5 W launched into a standard SMF.

Both references ([12], [18]) identify and exploit four-wave mixing (FWM) as the driving mechanism behind the data-processing capability of their systems. However, due to a pulsed input resulting from information encoding in the comb lines (cf. [19]) and SMF anomalous group-velocity dispersion (GVD), a variety of solitonic waves (single solitons and Akhmediev breathers) and their interactions such as soliton molecules, crystals, and gas is expected to evolve in the SMF ([20], [21], [22], [23], [24], [25], [26]) effectively reducing FWM ([27]) and, thus, data-processing capabilities of the ELM. On the other hand, Refs. [28], [29] discuss and show that solitons play a crucial role in data processing. As FWM and solitonic wave formation go hand in hand in optical fibers, they are difficult to separate for ELM optimization. Below, we will see that Shannon entropies of the optical power and phase allow for optimization of the ELM by taking the parameters of maximum and upper moderate entropy values, all this without knowing the precise dynamics.

I emulate the ELM on the computer and use numerical simulations to generate the ELM outputs. For the transformation of the encoded frequency comb in the ELM SMF, I use the Nonlinear Schrödinger Equation (NLS) for the optical field amplitude $A(z, t)$ in the slowly varying envelope approximation in the co-moving frame [27]: $\frac{\partial A}{\partial z} = -i\frac{\beta_2}{2}\frac{\partial^2 A}{\partial t^2} + i\gamma|A|^2A$ with $\beta_2 = -23$ ps²/km being the GVD parameter and $\gamma = 1.2$ W⁻¹ · km⁻¹ the nonlinear coefficient at $\lambda_0 = 1554.6$ nm (cf. [12]). The optical losses, higher-order dispersion, Raman effect, and shock of short pulses usually present in standard fibers are omitted as they have a negligible impact for SMF lengths considered here, ($L \leq 5$ km). The initial condition $A(z = 0, t)$ of the unmodulated comb provided by PM reads as: $A(z = 0, t) = \sqrt{P_0} \exp(i\omega_0 t + im \cos(2\pi\Omega t))$ with PM modulation frequency $\Omega = 15.625$ GHz and modulation depth $m = 1$. The temporal window chosen for simulations is 256 ps.

The bench dataset used here is the Iris dataset (4 features per sample) under the Min-Max normalization. Each input data sample \mathbf{x}^j is the duplication of the corresponding normalized Iris dataset sample such that the symmetric encoding (SYM) preserves the symmetry of the input comb shape, i.e. $\mathbf{x}^j = [x_1^j, x_2^j, x_3^j, x_4^j, 1, x_4^j, x_3^j, x_2^j, x_1^j]$, whereas the asymmetric encoding (ASYM) breaks the symmetry: $\mathbf{x}^j = [x_1^j, x_2^j, x_3^j, x_4^j, 1, x_1^j, x_2^j, x_3^j, x_4^j]$ (Fig. 1, bottom). The lines of the unmodulated comb are then attenuated according to these values (cf. [12]). Symmetric encoding reduces the average optical power by ca. 39% and the asymmetric one by ca. 29%.

The classification accuracy results presented below were obtained by randomly splitting the Iris dataset into 2/3-part for the training set and 1/3-part for the test set and performing a 10-fold cross-validation. The linear-regression regularization parameter λ is set to zero, i.e. $\lambda = 0$, to focus on physical ELM parameters rather than trying to achieve the best possible prediction. Therefore, the classification prediction values I achieve are usually lower than those achieved by state-of-the-art computer-based machine learning models or other comparable

neuromorphic photonics implementations. These values can be increased, though, by introducing and optimizing $\lambda > 0$.

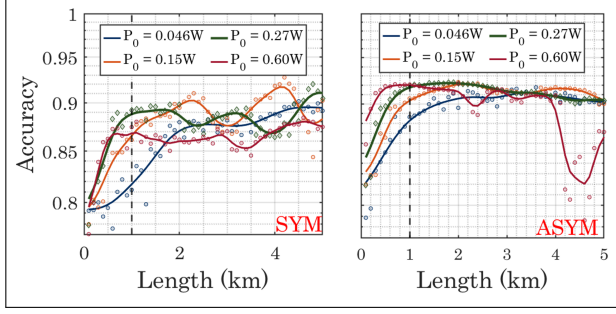


Fig. 2. Classification accuracy for Iris dataset over the fiber length of $L = 5$ km for symmetric (SYM) and asymmetric (ASYM) information encoding and different values of input power P_0 .

For Shannon entropy of the optical power averaged over N samples arbitrarily drawn from the Iris dataset, I write (cf. [16]):

$$E_{\text{pow}}(z) = -\frac{1}{N} \sum_{i=1}^N \int_{-128 \text{ ps}}^{128 \text{ ps}} |A_i(z, t)|^2 \log(|A_i(z, t)|^2) dt. \quad (1)$$

In the same manner, I define Shannon entropy of the optical phase:

$$E_{\text{phase}}(z) = -\frac{1}{N} \sum_{i=1}^N \int_{-128 \text{ ps}}^{128 \text{ ps}} \phi_i(z, t)^2 \log(\phi_i(z, t)^2) dt \quad (2)$$

with phase $\phi_i(z, t) = \text{atan2}(\Im(A_i(z, t)) / \Re(A_i(z, t)))$. For Shannon entropy of the optical spectrum, I write with Fourier transform \mathcal{F} :

$$E_{\text{spec}}(z) = -\frac{1}{N} \sum_{i=1}^N \int_{-0.5 \text{ THz}}^{0.5 \text{ THz}} |\mathcal{F}(A_i)|^2 \log(|\mathcal{F}(A_i)|^2) d\nu. \quad (3)$$

In all three equations, Eqs. 1, 2, 3, the integral limits reflect the system specifications. Theoretically, these limits are $\pm\infty$. Please note: whereas it might take up to several days to produce the ELM outputs as presented in Figs. 2, 4, top, using modern multicore computers, the calculation of the averaged entropies (Eqs. 1, 2, 3) might be a matter of few hours only depending on the sampled subset of the data. Below, we will see that the number of samples of only $N = 9$ (3 samples per Iris class) is sufficient to find optimal parameters of the ELM (Fig. 3, Fig. 4, bottom).

Results and Discussion. Fig. 2 shows the ELM classification accuracies for four different input powers ($P_0 = 0.046$ W, 0.15 W, 0.27 W, and 0.6 W), GVD parameter $\beta_2 = -23$ ps²/km, and nonlinear coefficient $\gamma = 1.2$ (W · km)⁻¹, as well as two types of information encoding, SYM and ASYM. For SMF length of $L \leq 1$ km, we see a rapid increase of classification accuracy with increasing input power for both types of information encoding. For SYM and $L > 1$ km, the accuracy curves exhibit oscillating behavior and even a decrease of the performance for $P_0 = 0.6$ W. For ASYM and $L > 1$ km, the accuracy curves are more well-behaving being smoother and reaching higher values (up to 0.925) than for SYM. However, we observe a dip in the accuracy for $P_0 = 0.6$ W with a minimum at around $L = 4.5$ km. These observations indicate that we deal with complex (but different)

dynamics for SYM and ASYM, with ASYM performing better than SYM in data processing capability.

Shannon entropy of the optical power (Eq. 1) is shown in Fig. 3, column one. We see that the entropy increases towards its maximum in yellow with input power in quite short SMF lengths ($L < 2$ km) for SYM and ASYM. Specifically for $L < 1$ km, a comparison with Fig. 2 reveals that higher entropy denotes a faster increase in accuracy. For fixed input powers, a decrease in entropy over the fiber length coincides with a decrease in the ELM classification performance. In particular, it is well seen for ASYM at $P_0 = 0.6$ W, where the drop in power entropy goes along with the dip in the ELM classification accuracy. From these observations, I conclude that Shannon entropy of the optical power can be used as a handy tool for quick estimation of the best parameters. Thus, we want system parameters where the power entropy is as high as possible (maximal or upper moderate) and avoid its decrease. Maximum power entropy (yellow) is achieved for input powers $P_0 = 0.5 - 0.6$ W and SMF lengths $L < 2.2$ km for SYM and $P_0 = 0.32 - 0.6$ W and SMF lengths $L < 2.1$ km for ASYM.

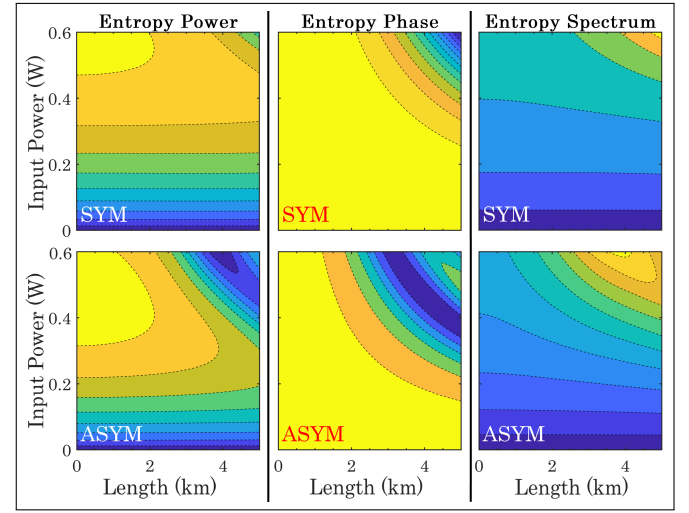


Fig. 3. Shannon entropy of optical power in W^2 , phase in rad^2 , and optical spectrum in $(\text{power spectral density})^2$ for SMF length of $L = 5$ km, different input powers P_0 , and information encoding types SYM and ASYM, all averaged over $N = 9$ arbitrary samples. The increase in the values goes from violet/dark blue (minimum) to yellow (maximum).

The entropy of the optical phase (Eq. 2, Fig. 3, column two) gives us a better orientation of what parameter space is to avoid for better ELM classification performance. These plots can be considered better-resolved representations of the critical regions compared to the case of the power entropy. These regions are denoted by a decrease of the phase entropy. They start for lower values of the SMF length and input power P_0 for both, SYM and ASYM as compared to Shannon entropy of the optical power. This effectively reduces the parameter range of good ELM performance. At the same time, the search for optimal parameters becomes more focused with maximal phase entropy as a target. With Shannon entropy of the optical phase as an auxiliary tool to power entropy, we reduce the SMF lengths to $L < 2.1$ km for SYM and $L < 1.2$ km for ASYM for any input power considered.

Fig. 3, column three, shows the Shannon entropy of the spectrum. Here, the entropy values are small for the least broad

frequency combs and increase towards the parameters delivering the broadest possible combs (plots of frequency combs omitted here). Although those are the parameters we should avoid when optimizing the ELM, they are useful from the perspective of the frequency-comb generation. Thus, this type of entropy might be interesting for the nonlinear optics community.

To accommodate both types of information encoding, SYM and ASYM, the maximal entropies of power and phase are given for the SMF length $L < 1.2$ km and input power $P_0 = 0.32 - 0.6$ W. These values will provide the fastest increase of the accuracy curves over the SMF length. However, Shannon entropies of the optical power and phase do not fully depict ELM's poor performance for $P_0 = 0.60$ W (SYM). To account for this fact, more studies and possibly other approaches are needed. I, therefore, go for slightly moderate entropies (rather than maximal ones) that still coincide with good ELM performance and choose $L = 1$ km and $P_0 = 0.27$ W for SYM and ASYM.

Fig. 4, top, shows the ELM classification accuracy curves for different values of the GVD parameter β_2 and a fixed value of input power $P_0 = 0.27$ W. For SYM, we see that the accuracy curves increase with the absolute value of β_2 which indicates more solitonic-waves-based information processing in the ELM (cf. [28]). For ASYM, there is no dependence of the accuracy on the value of β_2 . This observation supports the theory of FWM driving the data processing in the ELM (cf. [12], [18]). Black curves ($\gamma = 0$ ($\text{W} \cdot \text{km}^{-1}$)) depict the worst possible ELM performance and show that the Kerr nonlinearity is indeed needed for the ELM to perform well. Fig. 4, bottom, shows the corresponding Shannon entropies of the optical power. Yet again, we see that the ELM accuracy increases for system parameters where power entropy has its maximum (yellow) or upper moderate value (orange) and starts stagnating (ASYM) or shows an oscillatory behavior (SYM) for the regions of the decreasing power entropy (starting from green). This happens for $\beta_2 = -(3 - 23)$ ps^2/km and $L = 2.5 - 5$ km for SYM $\beta_2 = -(4 - 25)$ ps^2/km and $L = 2.2 - 5$ km for ASYM. This is another example that Shannon entropy of optical power can be used as a quick estimator of optimal system parameters of a fiber-based frequency-multiplexed ELM.

Conclusion. I consider a frequency-multiplexed fiber-based Extreme Learning Machine as an example for a classification task. I use Shannon entropy for the optical power and introduce Shannon entropy of the phase and spectrum, all averaged over a subset of the dataset under study, and show that maximal or upper moderate power and phase entropies coincide with the best ELM performance. Spectrum entropy provides parameter space for broadest possible frequency combs.

Funding. Project Win4Space / Win4ReLaunch (SPW EER Wallonie Belgique, grant agreement number 2210181).

Acknowledgments. The author acknowledges inspiring conversations about possible dependence between the ELM dynamics and its performance with Michael Böhm (Wismar University of Applied Sciences) and Serge Massar (Université libre de Bruxelles).

Disclosures. I declare no conflict of interest.

Data availability. Data underlying the results presented in this paper are not publicly available at this time but may be obtained from me upon reasonable request.

REFERENCES

1. P. L. McMahon, Nat. Rev. Phys. **5**, 717 (2023).
2. Y. Bai, X. Xu, M. Tan, *et al.*, Nanophotonics **12**, 795 (2023).

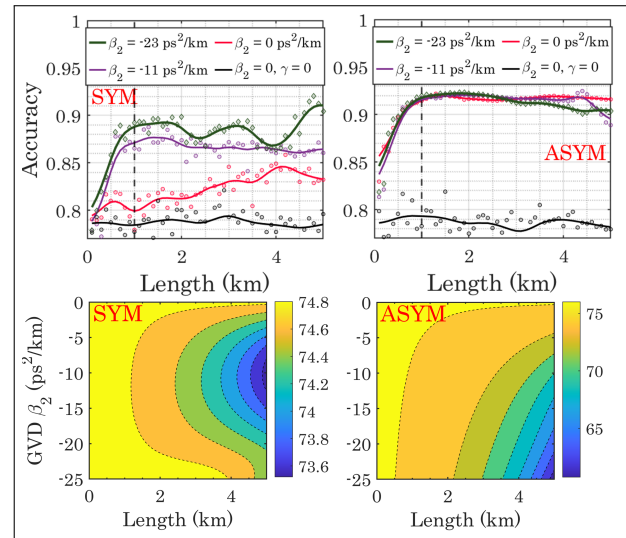


Fig. 4. Top: Classification accuracy for Iris dataset over the fiber length of $L = 5$ km for symmetric (SYM) and asymmetric (ASYM) information encoding, input power $P_0 = 0.27$ W, and different values of GVD parameter β_2 . The black curves serve as a reference for worst possible ELM performance. Bottom: Corresponding Shannon entropy of the optical power for SYM and ASYM.

3. X. Xu, W. Han, M. Tan, *et al.*, IEEE J. Sel. Top. Quantum Electron. **29**, 1 (2023).
4. J. Pauwels, G. Verschaffel, S. Massar, and G. Van der Sande, Front. Phys. **7** (2019).
5. G.-B. Huang, Cogn. Comput. **6**, 376 (2014).
6. Silva, Duarte, Ferreira, Tiago, Moreira, Felipe C., *et al.*, J. Eur. Opt. Soc. Publ. **19**, 8 (2023).
7. A. Lupo, L. Butschek, and S. Massar, Opt. Express **29**, 28257 (2021).
8. B. Fischer, M. Chemnitz, Y. Zhu, *et al.*, Adv. Sci. **10**, 2303835 (2023).
9. T. Zhou, F. Scalzo, and B. Jalali, J. Light. Technol. **40**, 1308 (2022).
10. M. Yildirim, I. Oguz, F. Kaufmann, *et al.*, APL Photonics **8**, 106104 (2023).
11. I. Oguz, J. Ke, Q. Weng, *et al.*, Opt. Lett. **48**, 5249 (2023).
12. M. Zajnulina, A. Lupo, and S. Massar, Opt. Express (2024).
13. P. M. Cincotta, C. M. Giordano, R. Alves Silva, and C. Beaugé, Phys. D: Nonlinear Phenom. **417**, 132816 (2021).
14. A. Lozano-Durán and G. Arranz, Phys. Rev. Res. **4**, 023195 (2022).
15. I. G. Sprinkhuizen-Kuyper, "Some remarks on the entropy of a neural network," (BENELEARN-96, 1996).
16. T. Yamano, The Eur. Phys. J. Plus **139**, 595 (2024).
17. F. Lima, Ann. Phys. **442**, 168906 (2022).
18. K. Sozos, S. Deligiannidis, C. Mesaritakis, and A. Bogris, IEEE J. Quantum Electron. **60**, 1 (2024).
19. C. Finot, Opt. Lett. **40**, 1422 (2015).
20. J. M. Dudley, G. Genty, F. Dias, *et al.*, Opt. Express **17**, 21497 (2009).
21. B. Frisquet, B. Kibler, and G. Millot, Phys. Rev. X **3**, 041032 (2013).
22. G. Xu, A. Gelash, A. Chabchoub, *et al.*, Phys. Rev. Lett. **122**, 084101 (2019).
23. U. Andral, B. Kibler, J. M. Dudley, and C. Finot, Wave Motion **95**, 102545 (2020).
24. R. Schiek, Opt. Express **29**, 15830 (2021).
25. M. Zajnulina and M. Böhm, Opt. Lett. **49**, 3894 (2024).
26. P. Suret, S. Randoux, A. Gelash, *et al.*, Phys. Rev. E **109**, 061001 (2024).
27. G. P. Agrawal, Nonlinear Fiber Optics (Academic Press, 2019), 6th ed.
28. G. Marucci, D. Pierangeli, and C. Conti, Phys. Rev. Lett. **125**, 093901 (2020).
29. A. Bile, H. Tari, R. Pepino, *et al.*, EPJ Web Conf. **287**, 13003 (2023).